July 1 (Wed)	Room A	Room B	Room C	Room D	Room E	Room F	Room G	Room H	Lobby, 2F
	Grand Ballroom 1, 2F	Grand Ballroom 2, 2F	Grand Ballroom 3, 2F	Capri, 2F	Sydney, 2F	Sicily, 1F	Miami, 2F	Venice, 2F	
08:30-10:00	We1A	We1B	We1C	We1D	We1E	We1F	We1G		Exhibition
	PCS and FEC Coding Technologies	Fiber Lasers	Converged Fiber-Wireless & RoF Systems	Technologies for Coherent Short-Reach Transmission	Nonlinear & Active Integrated Photonics	III-V on Silicon Active Devices II & Electronic ICs	Quantum Communication and Networking		
10:00-11:45	Poster Session III (Grand Ballroom 4, 2F)								
11:45-13:15	Lunch (on your own)								
13:15-14:45	We2A	We2B	We2C	We2D	We2E	We2F	We2G		
	Advanced Lasers	Multimode & Multicore Fibers	Satellite Optical Communication	Radio-over-Fiber and Optical Wireless Systems	Scalable Silicon Photonics Platforms	Datacom & VCSELs	Optoacoustic and Coherent Detection Technologies		
14:45-15:00	Coffee Break								
15:00-16:30				We3D	We3E	We3F	We3G		
				Advanced DSP for Transmission and Sensing	Nonlinear & Spectral Integrated Photonics	Coherent Communications & Novel Sources	Multi-modal Optical Technologies for Imaging and Sensing		
16:30-16:45	Coffee Break								
16:45-18:30				PDP Session1	PDP Session2				
18:30-21:00	Banquet (Grand Ballroom, 2F)								

Room F (Sicily), 2F | Chair: Chih-Hsien Cheng (NICT)

We2F July 1 (Wed), 2026
Datacom & VCSELs 13:15-14:45

We2F-1 **13:15-13:30**

ntegrated Wavelength Division Multiplexing Transmitter with Dispersion Pre-compensation

Weihan Wang, Ruitao Ma, Fei Huang, Mingyu Zhu, Aoyun Gao, Zexu Wang, Shujun Liu, Weike Zhao, Yiwei Xie, Zejie Yu, Daoxin Dai
Zhejiang University

We2F-2 **13:30-13:45**

3–300 K 850 nm VCSEL for Cryogenic Optical Interconnects with 128 Gbps PAM-4 at 3 K

Etina Zou1, Zetai Liu2, Min-Hsin Wu1, Chung-Hsin Yu1, Yun-Cheng Yang1, Milton Feng2, Chao-Hsin Wu1
[1]National Taiwan University, [2]University of Illinois Urbana-Champaign

We2F-3 **13:45-14:00**

High-Bandwidth-Density 850 nm VCSEL Array for Terabit Optical Interconnects

Min-Hsin Wu, Etina Zou, I-Chi Liu, Yun-Cheng Yang, Chao-Hsin Wu
National Taiwan University

We2F-4 **14:00-14:15**

A 2-λ × 50-Gb/s PAM-4 Silicon RingResonator-Based WDM Optical Receiver

Jae-Ho Lee[1], Dong-Hyeon Kim[1], Yongjin Ji[1], Seung-Jae Yang[1], Hyun-Kyu Kim[2], Woo-Young Choi[1]
[1]Yonsei Universit, [2]Samsung Electronics Co., Ltd.

We2F-5 **Invited** **14:15-14:45**

Zn-Diffusion Single-Mode VCSELs at 850 and 1060 nm for High-Speed AI Interconnection

Jin-Wei Shi
National Central University

A 2-λ × 50-Gb/s PAM-4 Silicon Ring-Resonator-Based WDM Optical Receiver

Jae-Ho Lee*, Dong-Hyeon Kim*, Yongjin Ji*, Seung-Jae Yang*, Hyun-Kyu Kim**, and Woo-Young Choi*
* Department of Electrical and Electronic Engineering, Yonsei University, Seoul, Republic of Korea
** Formerly at Yonsei University when this work was done. Now at Samsung Electronics, Hwaseong, Republic of Korea

Abstract

We demonstrate a 2-λ × 50-Gb/s PAM-4 silicon (Si) ring-resonator-based wavelength division multiplexing (WDM) optical receiver. Each optical receiver achieves BER less than 1e-12 for 32-Gb/s NRZ and less than 2.4e-4 for 50-Gb/s PAM-4 data.

I. Introduction

The explosive growth of artificial intelligence (AI) and high-performance computing (HPC) systems demands high-bandwidth data communications. As systems scale out, conventional electrical interconnects have limitations in increasing data throughput with high energy efficiency. As a result, optical interconnects are increasingly used to meet the required data throughput. Si photonics is widely adopted due to its compatibility with complementary metal-oxide-semiconductor (CMOS) process and a great potential for large-scale integration. Among various Si photonic devices, ring resonators offer small footprints and high wavelength selectivity, making them suitable for WDM systems by cascading multiple ring resonators [1]. For the receiver operation, ring resonator filters (RRFs) are used to demultiplex WDM channels.

In this paper, we present the hybrid-integrated 2-λ × 50-Gb/s PAM-4 Si RRF WDM optical receiver. The proposed optical receiver achieves a bit error rate (BER) less than 2.4e-4 at an input optical modulation amplitude (OMA) of -7.49-dBm without any pulse pattern generator (PPG) and bit error rate tester (BERT) equalization.

II. System Implementation

Fig. 1 shows a block diagram of the implemented WDM optical receiver and its external temperature controller (TC). The WDM optical receiver consists of a photonic IC (PIC), an electronic IC (EIC) and its photograph is shown in Fig. 2. The PIC is fabricated by Advanced Micro Foundry and consists of two RRFs with the same geometry sharing a single bus waveguide. Each RRF has a metal heater to tune its resonance wavelength and a germanium-photodetector (PD) integrated at its drop port, whose output is wire-bonded to the EIC. In addition, the PD cathode voltages are supplied with 2.6-V using low-dropout regulators (LDOs) in the EIC. The EIC is fabricated by Samsung 28-nm CMOS technology and consists of two inverter-based receivers with inductive peaking.

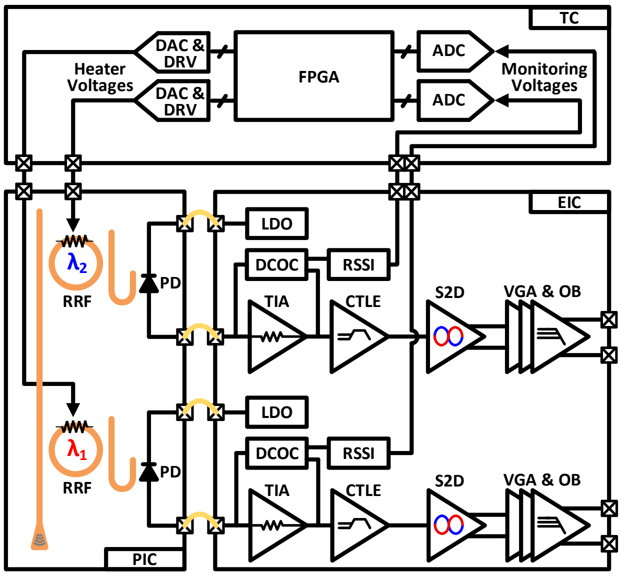

Fig. 1. Block diagram of the WDM optical receiver with external TC.

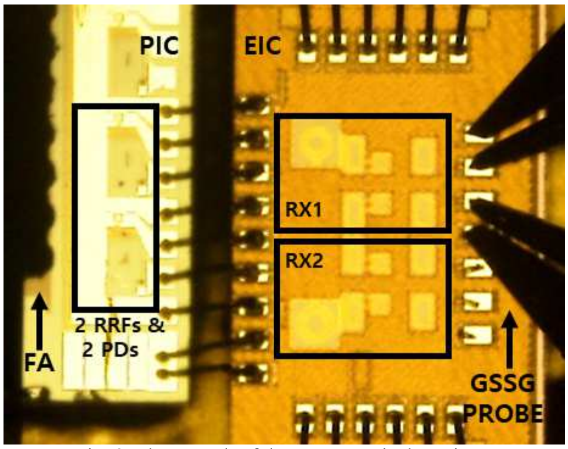

Fig. 2. Photograph of the WDM optical receiver.

Each receiver has a transimpedance amplifier (TIA), a continuous time linear equalizer (CTLE), a single-to-differential amplifier (S2D), variable gain amplifiers (VGAs), and a 50-ohm output buffer (OB). A DC offset cancellation (DCOC) loop removes DC currents from the PD and a received signal strength indicator (RSSI) monitors received average optical power. The TC consists of two 8-bit ADCs, two 8-bit DACs with heater drivers (DRVs) and a field-programmable gate array (FPGA). The TC sweeps the heater voltage of each RRF to align its resonance wavelength with the input wavelength by maximizing each RSSI output voltage. The resonance wavelength locking of each RRF is maintained using a dither-and-track technique reported in our previous work [2].

This work was supported by the Institute of Information & Communications Technology Planning & Evaluation (IITP) grant funded by the Korea government (MSIT) (No. RS-2025-09942968, AI Semiconductor Innovation Lab (Yonsei University) and RS-2025-02304291).

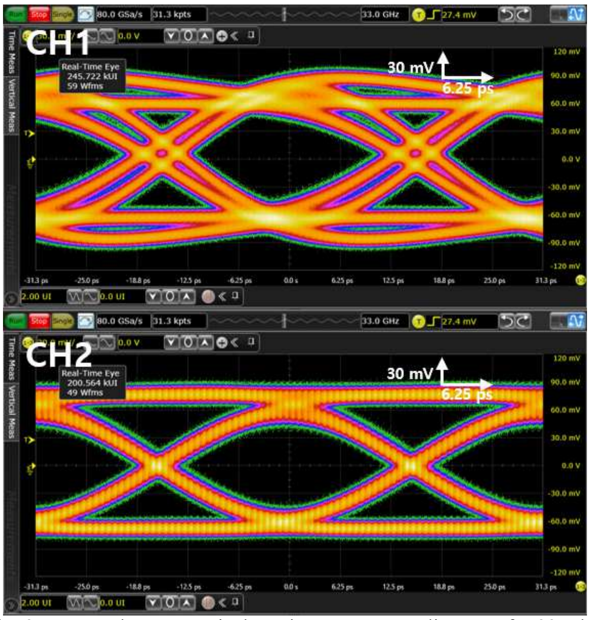

Fig. 3 Measured WDM optical receiver output eye diagrams for 32-Gb/s PRBS-31 NRZ input data.

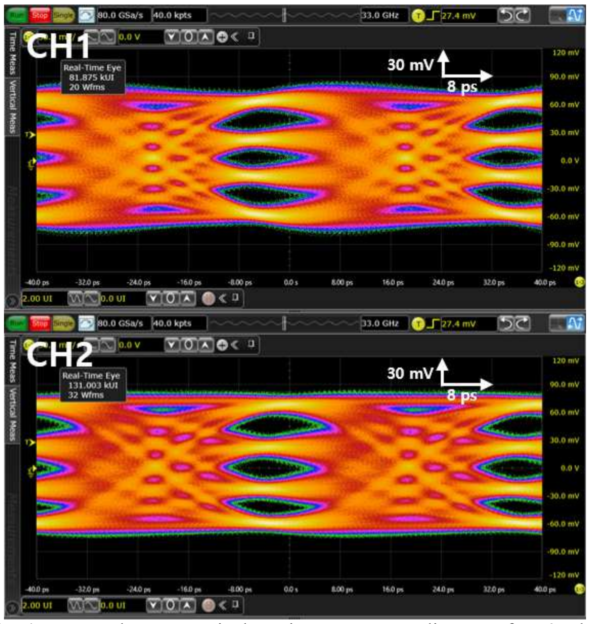

Fig. 4 Measured WDM optical receiver output eye diagrams for 50-Gb/s PRBS-15 PAM-4 input data.

III. Measurement Results

To evaluate the WDM optical receiver operation, the hybrid-integrated optical receiver is packaged on an FR4 PCB and measured at 25-°C by using a temperature-controllable stage. Two different input wavelengths of λ_1 = 1530.0-nm and λ_2 = 1531.6-nm are combined through the 2 by 1 fiber coupler and coupled into the PIC through a fiber array (FA). Due to the limitations in our measurement setup, only one input wavelength can be modulated with pseudo-random binary sequence (PRBS) data using a Mach-Zehnder modulator. An erbium-doped fiber amplifier (EDFA) is used to compensate for fiber insertion loss, followed by a variable optical attenuator (VOA) to adjust the incident optical power. The heater driver operates with 2.2-V supply voltage, which enables resonance wavelength tuning beyond one free spectral range of each RRF. The receiver outputs are measured using GSSG RF probes.

Fig. 3 shows the measured 32-Gb/s PRBS-31 NRZ output eye diagrams of the WDM optical receiver. Fig. 4 shows the measured 50-Gb/s PRBS-15 PAM-4 output eye diagrams of the WDM optical receiver. Eye diagrams are measured without PPG and oscilloscope equalizations, while the TC is in dither-and-track mode. The difference in the measured eye diagrams between channel1 (CH1) and channel2 (CH2) originates from the difference in the TIA inductor sizes to examine their impact on the overall response.

Fig. 5 shows the measured BER curves of the WDM optical receiver as a function of input OMA. For 32-Gb/s PRBS-31 NRZ input data, the BER less than 1e-12 is achieved at the input OMA of -10.6-dBm. For 50-Gb/s PRBS-15 PAM-4 input data, the BER less than the pre-FEC limit of 2.4e-4 is achieved at the input OMA of -7.49-dBm. Each WDM receiver consumes 58.7-mW from a 1.25-V supply voltage, achieving energy efficiency of 1.17-pJ/bit for the 50-Gb/s PAM-4 operation.

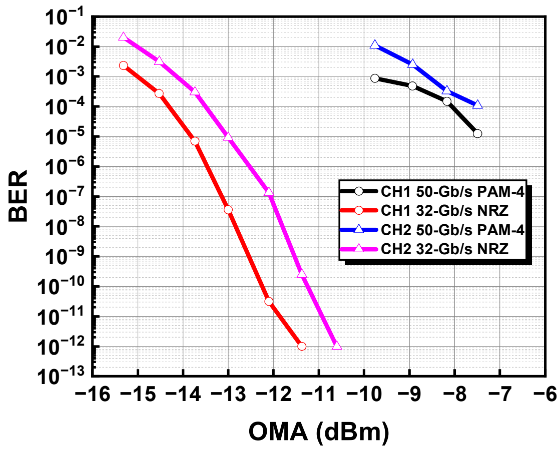

Fig. 5 Measured BER curves of the WDM optical receiver for 32-Gb/s PRBS-31 NRZ and 50-Gb/s PRBS-15 PAM-4 input data.

IV. Conclusion

We demonstrate the hybrid-integrated 2-λ × 50-Gb/s PAM-4 Si RRF WDM optical receiver, which achieves BER less than 2.4e-4 at the input OMA of -7.49-dBm without any equipment equalization.

Acknowledgment

Jae-Ho Lee and Dong-Hyeon Kim contributed equally to this work. The chip fabrication was supported by the Samsung Electronics and the EDA tool was supported by the IC Design Education Center (IDEC), Korea.

References

[1] P. Bhargava et al., “A 256Gbps Microring-Based WDM Transceiver with Error-Free Wide Temperature Operation for Co-Packaged Optical I/O Chiplets,” in *Proc. IEEE Symp. VLSI Technol. Circuits*, Jun. 2024, pp. 1-2.

[2] H.-K. Kim et al., “A 4-λ × 28-Gb/s/λ Silicon Ring-Resonator-Based WDM Receiver With a Reconfigurable Temperature Controller,” *J. Light. Technol.*, vol. 42, no. 7, pp. 2296–2302, Apr. 2024.